Effects of Mutant Rat Dynamin on Endocytosis

Jonathan S. Herskovits,* Christopher C. Burgess, Robert A. Obar, and Richard B. Vallee

Cell Biology Group, The Worcester Foundation for Experimental Biology, Shrewsbury, Massachusetts 01545; and
*Department of Biochemistry, University of Massachusetts Medical School, Worcester, Massachusetts 01655

Abstract. Dynamin is a 100-kD microtubule-activated GTPase. Recent evidence has revealed a high degree of sequence homology with the product of the *Drosophila* gene *shibire*, mutations in which block the recycling of synaptic vesicles and, more generally, the formation of coated and non-coated vesicles at the plasma membrane. We have now transfected cultured mammalian COS-7 cells with both wild-type and mutant dynamin cDNAs. Point mutations in the GTP-binding consensus sequence elements of dynamin equivalent to dominant negative mutations in ras, and an NH₂-terminal deletion of the entire GTP-binding domain of dynamin, block transferrin uptake and alter the distribution of clathrin heavy chain and α-, but not γ-, adaptin. COOH-terminal deletions reverse these effects, identifying this portion of dynamin as a site of interaction with other components of the endocytic pathway. Over-expression of neither wild-type nor mutant forms of dynamin affected the distribution of microtubules. These results demonstrate a specific role for dynamin and for GTP in the initial stages of receptor-mediated endocytosis.

D YNAMIN was discovered in microtubule preparations as a 100-kD nucleotide-sensitive microtubule-binding protein (Shpetner and Vallee, 1989). Molecular cloning of rat brain dynamin revealed it to contain the three well-conserved consensus sequence elements characteristic of almost all known GTP-binding proteins (Obar et al., 1990). Dynamin was subsequently found to have a GTPase activity which can be potently activated by microtubules (Shpetner and Vallee, 1992).

Dynamin was found to be related in sequence to several other proteins (Obar et al., 1990). These include the vertebrate Mx proteins, which are induced by interferon, and confer resistance to myxoviral infection (Horisberger et al., 1983, 1990; Staeheli et al., 1986); VPS1p, the product of the *Saccharomyces cerevisiae* VPS1/SPO15 gene, involved in sorting of proteins from the Golgi apparatus to the yeast vacuole and in meiotic chromosome segregation (Rothman et al., 1989; Yeh et al., 1991); and the product of the *S. cerevisiae* MGM-1 gene, involved in mitochondrial reproduction (Jones and Fangman, 1992). These proteins show a particularly high degree of sequence homology with dynamin within the NH₂-terminal 300 amino acids, the region containing the GTP-binding consensus sequence elements. However, despite the clear similarity in primary structure between the members of this newly emerging class of proteins, their functional relationship remains elusive.

Recently, the product of the well known *shibire* gene in

Drosophila has also been shown to be related to dynamin (Chen et al., 1991; van der Bliek and Meyerowitz, 1991). In contrast to the other proteins in this class, the *shibire* gene product shows a high degree of sequence identity to rat dynamin (68%) throughout its length, has an almost identical molecular weight, and shares a basic, proline-rich COOH-terminal domain absent in the other dynamin-related proteins.

shiᵗˢ mutants were initially isolated in a screen for temperature-sensitive paralytic flies (Grigliatti et al., 1973). The paralytic defect was traced to a dysfunction at the neuromuscular junction and other synapses in the reformation of synaptic vesicles following neurotransmitter release (Poodry and Edgar, 1979; Kosaka and Ikeda, 1983a; Koenig et al., 1983). Further work revealed that *shiᵗˢ* mutants are generally deficient in a very early step in endocytosis, the ability to form coated as well as non-coated vesicles at the plasma membrane, and are completely blocked in the ability to take up fluid phase endocytic markers (Kosaka and Ikeda, 1983b; Kessel et al., 1989; Masur et al., 1990). The similarity between *shi* and rat dynamin in primary structure and the ability of both proteins to bind to microtubules (Chen et al., 1991) suggests that they are closely related in function, but no direct evidence exists as yet implicating the mammalian protein in a role in the endocytic pathway.

The present study was undertaken to gain insight into the physiological role of mammalian dynamin. Wild-type and mutant dynamin constructs were transfected into COS-7 cells to determine the distribution of the protein, which has been difficult to evaluate by traditional immunocytochemistry, and to begin to define the role of GTP-hydrolysis in its mechanism of action. Our results indicate that dynamin is a

---

soluble GTPase which interacts with particulate structures during its GTPase cycle. Mutations in the GTP-binding domain result in dominant inhibition of receptor-mediated endocytosis, and alter the distribution of plasma membrane- but not Golgi-derived clathrin assembly proteins. Finally, we find the COOH-terminal portion of dynamin to play a critical role in its cellular activities.

Materials and Methods

Antibodies

Two rabbit polyclonal antibodies to distinct regions of rat dynamin were used for this study. One, termed R2, directed against a bacterially expressed, glutathione-S-transferase fusion protein encoding the NH_2-terminal 651 amino acids of rat brain dynamin has been previously described (Chen et al., 1991, 1992). An additional antibody, termed RA, was produced against a synthetic peptide corresponding to the COOH-terminal 20 amino acids of rat brain dynamin (NH2-Cys-Gly-VPSRPNRAPPGVPRITI-SDP-COOH). The peptide was conjugated to KLH and injected using the MPL + TDM + CWS adjuvant (RIBI Immunochemical Research, Hamilton, CT) into rabbits at multiple subcutaneous sites. The R2 antibody was blot affinity purified (Olmsted, 1981) against bovine brain dynamin. The RA antibody was used either after similar blot affinity purification, or as an IgG fraction produced by Protein A-Agarose (Bio-rad Laboratories, Palo Alto, CA) chromatography as noted. Immunoreactivity with the RA antibody was completely abolished by pre-adsorption with 5 μg/ml of peptide for 10 min.

Despite the absence of tubulin from bacterially expressed dynamin and the lack of tubulin reactivity on immunoblots, the affinity-purified R2 antibody produced a microtubule staining pattern, curiously recognizing only the distal portions of the microtubules. Adsorption of the antibody against purified tubulin (presented as taxol-stabilized microtubules) eliminated staining without affecting dynamin reactivity on immunoblots, and was, therefore, routinely performed prior to use of the R2 antibody for immunofluorescence microscopy. Whatever the explanation for these observations, the RA anti-peptide antibody was used for most experiments, and the results were then checked using the R2 antibody.

The following antibodies to a variety of other antigens were also used during the course of this study: clathrin heavy chain (antibodies X-22, a gift of Dr. F. Brodsky (University of California, San Francisco, CA), and OZ-71, a gift of Dr. R. Anderson, University of Texas Southwestern Medical Center, Dallas, TX); α-adaptin (antibody ACM11, a gift of Dr. M. Robinson, University of Cambridge, Cambridge, UK); γ-adaptin (antibody 100.3, a gift of Dr. E. Ungewickell, Washington University, St. Louis, MO); Golgi 58-kD antigen (antibody K-9, a gift of Dr. G. Bloom, University of Texas Southwestern Medical Center); β-COP (antibody M3A5, a gift of Dr. T. Kreis, Sciences III, Geneva, Switzerland); and BiP (a gift of Dr. D. Bole, University of Michigan Medical Center, Ann Arbor, MI). Antibodies to β-tubulin and vimentin were purchased from Amersham, Ltd. (Arlington Heights, IL) and Sigma Chemical Co. (St. Louis, MO), respectively.

Expression Constructs and Site-directed Mutagenesis

The dynamin-1 full-length insert (Obar et al., 1989) was subcloned into the multiple cloning site of the pSVL mammalian expression vector (Pharmacia LKB Biotechnology, Piscataway, NJ). Point mutations were introduced using sequential PCR steps as described (Aruffo, 1991). All base substitutions were verified by dideoxy sequencing (Sanger et al., 1977). The deletion mutants were created from restriction fragments of the full-length constructs. Construct C-794 was created by deletion of a XmaI fragment from position 2425 of the dynamin insert to a XmaI site in the multiple cloning site (MCS)[1] of the pSVL vector and adds 10 amino acids from the vector sequence (ELGSRHDKIH) to the COOH terminus of the expressed dynamin molecule. Construct C-663 was created by deletion of a fragment from the BspEI site at position 2031 of the dynamin insert to the XmaI site in the MCS and adds six amino acids (GARIQT) to the COOH terminus of the expressed dynamin molecule. For the NH_2-terminal deletions, protein translation would begin at the amino acid indicated. Constructs N-272 and

1. *Abbreviations used in this paper*: BFA, brefeldin A; MCS, multiple cloning site.

N-651 were created by deletion of an EcoRV fragment and a NcoI fragment, respectively, of the dynamin-I insert in pBluescript followed by subcloning of the resultant deletion constructs into the pSVL vector. Construct N-435 was created by isolating a SacI fragment from the SacI site at position 1350 of the dynamin insert to the SacI site in the MCS of the pSVL vector. This SacI fragment was then inserted into a SacI cut pSVL vector. Plasmid DNA for transfections was prepared by the alkaline lysis method, followed by PEG precipitation, chloroform extraction, and reprecipitation with ethanol. Other methods were performed according to standard protocols. Expression levels of wild-type and mutant forms of dynamin were judged to be comparable by immunofluorescence. Expression levels varied, but we estimate on average ~100-fold overexpression based on total immunoprecipitable protein per culture dish and the fraction of transfected cells.

Cell Culture and Transfections

COS-7 cells (ATCC CRL 1651; American Type Culture Collection, Rockville, MD) were cultured in DME (GIBCO-BRL, Gaithersburg, MD) containing 10% FCS (Sigma Immunochemicals, St. Louis, MO), 100 U/ml penicillin, and 100 μg/ml streptomycin. The cells were maintained in a humidified 5% CO_2 atmosphere at 37°C. Transient transfections using DEAE-dextran were performed as described (Cormack, 1991) with the following modifications; 1) The day prior to transfection, the cells were seeded onto flame-sterilized coverslips, and 2) Opti-MEM Reduced-Serum Medium (Gibco/BRL) was used in place of DMEM-10NS. The cells were analyzed 48-72 hours after transfection.

Immunofluorescence Microscopy

For localization experiments other than those involving endocytosis, coverslips bearing transfected cells were rinsed briefly in PBS (137 mM NaCl, 2.7 mM KCl, 4.3 mM Na_2HPO_4, 1.4 mM KH_2PO_4, pH 7.4) and fixed for 5 min by immersion in −20°C methanol. 3.7% formaldehyde or 0.25% glutaraldehyde in PBS were used as alternative fixatives, followed by permeabilization with 0.1% Triton X-100, but neither fixative had an appreciable effect on the immunofluorescence pattern. The cells were rehydrated in TBS (50 mM TRIS/HCl, pH 7, 150 mM NaCl), blocked with 10% BSA in TBS, and incubated for 1 h at room temperature with either 1:200 protein A-purified RA or undiluted affinity-purified R2 as primary antibodies diluted in TBS containing 0.25% BSA with or without 0.05% NP-40. After four washes in TBS, the coverslips were incubated with a 1:100 dilution of affinity-purified secondary antibodies (fluorescein-conjugated sheep anti-mouse IgG and rhodamine-conjugated goat anti-rabbit IgG) (Organon Teknika-Cappel, Durham, NC). The coverslips were then washed four times with TBS and once with distilled water and mounted in gelvatol. Cells were observed by epifluorescence using a Zeiss Axioskop (Carl Zeiss, Thornwood, NY) and photographed using Kodak TMAX 400 film (Eastman Kodak, Rochester, NY).

The effects of the following treatments on the distribution of dynamin immunoreactivity in the transfected cells were assessed: Triton X-100 (0.5% in 50 mM Pipes, 12.5 mM Hepes, 4 mM EGTA, 1 mM MgSO$_4$, pH 7.0 for 5 min at 37°C); brefeldin A (5 μg/ml in DME for 3 min at room temperature); nocodazole (20 μg/ml in DME for 1 h at 37°C); taxol (10 μg/ml in DME for 2 h at 37°C; ATP depletion (10 mM sodium azide, 10 mM 2-deoxyglucose in DME for 2 h at 37°C).

Endocytosis Assays

COS-7 cells were preincubated for 30–60 min in serum-free medium (DME, GIBCO/BRL, Gaithersburg, MD) at 37°C, and then incubated in 20 μg/ml of FITC- or TRITC-transferrin or 3.3 mg/ml of FITC-conjugated lysine-fixable dextran (Molecular Probes, Eugene OR) at 37°C. The cells were washed briefly in PBS, fixed in 4% paraformaldehyde (EM grade; EMS, Fort Washington, PA) for 15 min, and then permeabilized with acetone for 5 min at −20°C or by inclusion of 0.02–0.2% saponin during the antibody incubations. For most experiments the cells were then labeled with anti-dynamin antibody (Protein A-Agarose–purified RA anti-peptide antibody diluted 1:300; or, where necessary due to the deletion of the dynamin COOH terminus, the R2 antibody prepared as described above), followed by rhodamine-conjugated goat anti-rabbit IgG, and observed by fluorescence microscopy as described above. For comparison of transferrin and dextran uptake, the permeabilization step was omitted.

SDS-PAGE and Immunoblotting

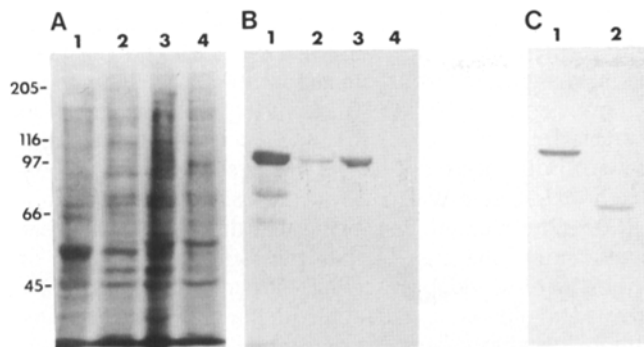Rat brain samples were homogenized in an equal volume of 0.1 M PEM

Figure 1. Immunoblotting with antibody against COOH-terminal dynamin peptide. Samples were electroblotted and stained with Ponceau S (*A*) or a 1:50 dilution of affinity-purified RA antibody. Samples were as follows: (*A* and *B*) lane *1*, adult rat brain; lane *2*, embryonic rat brain (E15); lane *3*, mouse 3T3 cells; and lane *4*, human A431 epidermoid carcinoma cells; (C) lane *1*, COS-7 cells transfected with rat dynamin construct K44E; and lane *2*, COS-7 cells transfected with rat dynamin construct N-272 which encodes a polypeptide lacking the first 271 amino acids. Construct K44E produced full-length protein while construct N-272 produced a truncated protein of ~66 kD. No reaction with endogenous COS-7 cell dynamin was observed using the RA anti-peptide antibody. Fragments of dynamin may be seen in the sample in B lane *1*.

buffer (Vallee, 1986) and solubilized in SDS–containing electrophoresis sample buffer. Cultured cells were suspended directly in 10 vol of sample buffer. Samples were loaded at roughly equal protein concentration as estimated by Ponceau S staining. Electrophoresis was conducted using 8% polyacrylamide (Laemmli, 1970), and electroblotting onto nitrocellulose according to Towbin et al. (1979). Following transfer, the nitrocellulose was stained with a 1:200 dilution of Ponceau S (Sigma Immunochemicals), destained in distilled water, and blocked in 5% nonfat milk in TBS containing 0.05% Tween-20. The blots were incubated in a 1:50 dilution of affinity-purified R2 or RA anti–peptide antibody followed by an alkaline phosphatase–conjugated secondary antibody (Promega, Madison, WI) and developed using NBT and BCIP.

Results

Immunological Characterization

To assay the distribution of endogenous and recombinant dynamin, we raised polyclonal antibodies to distinct regions of the molecule. Antibody R2 was generated against the amino-terminal two-thirds of rat brain dynamin (codons 1–651) and detected a strong-100 kD band in brain tissue (Chen et al., 1991). The R2 antibody showed broad species cross-reactivity, recognizing bands of ~100 kD in samples of *Drosophila*, mouse, hamster, cow, human, and yeast origin. The antibody did not recognize yeast VPS1p or bacterially expressed Mxl, and, thus, it does not seem to recognize the amino terminal sequences conserved between dynamin and the other members of its protein family.

Antibody RA was raised against a synthetic peptide corresponding to the COOH-terminal 20 amino acids of rat brain dynamin. It reacted with a 100-kD band in rat brain and mouse 3T3 cells, but not with human (A431 cells) or monkey (COS-7) cells (Fig. 1), consistent with the relatively limited sequence conservation at the COOH-terminal end of the molecule (cf. Chen et al., 1991; van der Bliek and Meyerowitz, 1991).

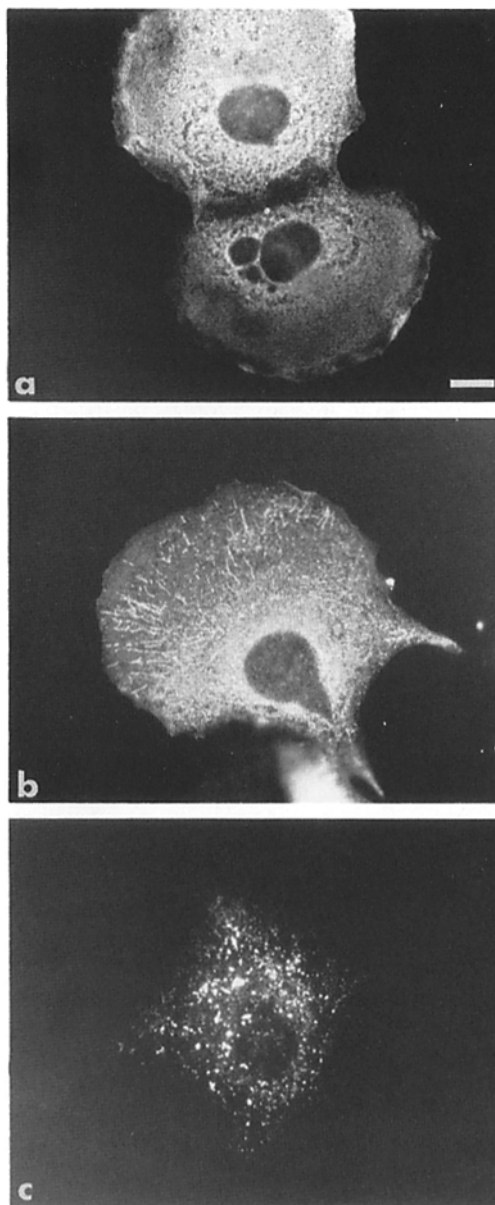Using either the R2 or RA anti–peptide antibody, initial attempts to define the distribution of dynamin by immuno-

Figure 2. Subcellular distribution of wild-type and mutant dynamin. COS-7 cells were transfected with (*a*) the wild-type dynamin construct D-1, seen expressed at different levels in two adjacent cells; (*b*) the point mutant construct K44E; and (*c*) the NH₂-terminal deletion construct N-272. The wild-type and mutant proteins were visualized using the protein A–purified RA anti-peptide antibody diluted 1:200. Note the diffuse cytoplasmic staining of a pair of cells expressing the wild-type protein in *a*; the punctate and linear structures in addition to the general diffuse staining in cells expressing the K44E point mutant protein; and the striking punctate structures in cells expressing the NH₂-terminally deleted protein. Bar, 10 μm.

fluorescence microscopy revealed only marginally detectable cytoplasmic staining in a variety of cell types examined, including 3T3, CHO, Rat-2, COS-7, and primary rat brain cells (and cf. Scaife and Margolis, 1990). This was despite the fact that the protein was detectable in all of these cell types by immunoblotting, and that recombinant dynamin could be readily detected under the fixation conditions used for immunocytochemistry (see below).

Localization of Wild-type and Mutant Dynamin

As an alternative approach to defining the subcellular distribution of dynamin, we transfected COS-7 cells with wild-type and mutant rat dynamin cDNAs. Approximately 10% of the cells were seen to express the rat protein over a wide concentration range as judged by immunofluorescence microscopy. Use of the RA anti–peptide antibody confirmed the expression of full-length protein (Fig. 1). It was also particularly useful in these studies in recognizing only the transfected rat dynamin (e.g., Fig. 1 C, lane 2).

Wild-type dynamin was observed to have a uniform distribution throughout the cytoplasm (Fig. 2 a). The staining pattern was not entirely featureless, but had a granular or mottled appearance. In general, distinct cytoplasmic structures such as microtubules, clathrin coated pits or vesicles, or other membranous organelles were not observed, though in occasional cells evidence of punctate staining could be seen through the predominant diffuse pattern. In general, recombinant wild-type dynamin was almost completely extractable before fixation with 0.5% Triton X-100, leaving a low level of weak, diffusely distributed protein. In some experiments, weak dynamin staining could be seen associated with microtubules following detergent extraction of the transfected cells, as judged by double labeling with anti-tubulin antibody. In these cases dynamin could also be observed on neighboring microtubules of adjacent cells, suggesting that microtubule binding occurred only after release of dynamin from the transfected cells and might represent a non-physiological interaction. Treatment of the transfected cells with nocodazole, brefeldin A (BFA), aluminum fluoride, or 2-deoxy glucose plus sodium azide to deplete cellular ATP had no detectable effect on the dynamin distribution (data not shown).

To gain further insight into the cellular role of dynamin and to identify functionally important domains of the molecule, a series of mutant constructs were generated (Tables I and II). All of the constructs were transfected into COS-7 cells and analyzed by immunofluorescence microscopy. To evaluate the effect of GTP hydrolysis on the distribution of dynamin, the point mutant constructs K44E and S45N were produced, with mutations in the first GTP-binding consensus sequence element (Tables I and II). Mutations at the equivalent sites in ras (K16 and S17) result in dominant inhibitory effects on cell growth and viability (Sigal et al., 1986; Feig and Cooper, 1988; Farnsworth and Feig, 1991). An additional point mutant construct, D208N, was produced in the third element of the tripartite GTP-binding consensus sequence (Tables I and II). A mutation at the equivalent position in ras (D119) is oncogenic (Feig et al., 1986; Sigal et al., 1986).

The immunofluorescent staining pattern obtained using constructs K44E (Fig. 2 b) and S45N (Fig. 3 b) generally differed from that for the wild-type construct (Fig. 2 a); in contrast, the pattern for construct D208N was indistinguishable from that for the wild-type construct (Fig. 3 d). Many of the cells transfected with K44E or S45N contained a large number of dynamin-positive spots and some contained brightly stained linear elements (see, especially, Figs. 2 b, 7 b, 8 b), though a diffuse background was still evident. The linear structures tended to be oriented radially and to be located near the margin of the cell. They were of variable length, but had a constant diameter of ~0.5 μm. Their ap-

pearance was reminiscent of tubular structures seen in shi[s] cells at restrictive temperature (e.g., Kessell et al., 1989), or in mammalian cells treated with BFA (Lippincott-Schwartz et al., 1990, 1991). A variety of experiments to characterize these structures were performed (data not shown): Both the spots and the linear elements were completely extractable with a 5-min exposure to 0.5% Triton X-100 before fixation, suggesting that they might represent membranous elements. Despite the radial arrangement of these structures, double labeling with anti-tubulin antibody revealed no obvious association with microtubules. Staining with the membrane-miscible reagent DiI (Honig and Hume, 1986; Flucher et al., 1991) or with wheat germ agglutinin revealed no apparent labeling of the linear structures, suggesting that they were not continuous extensions of the plasma membrane. Exposure of the cells to nocodazole, aluminum fluoride, or BFA, or depletion of ATP had no effect on the distribution or appearance of the linear structures. Their insensitivity to nocodazole indicated that they were likely to be distinct from BFA-induced structures (Lippincott-Schwartz et al., 1990). Under no conditions were the mutant forms of dynamin seen to co-localize with microtubules. Furthermore, double labeling with anti-tubulin revealed no apparent effect of the wild-type or mutant forms of dynamin on microtubule distribution.

To define more fully functionally important regions of the dynamin molecule, a number of deletion mutants were constructed (Table I). Construct N-272, which lacked the entire GTP-binding domain, showed an even more dramatic change in distribution from the wild-type dynamin pattern than seen with the point mutations (Fig. 2 c; see also Figs. 3 c, 7 c, 8 a). All of the protein expressed from the N-272 construct appeared to be present in bright spots with no evidence for a diffuse background of soluble protein. The spots varied in size, with many appearing larger and brighter than those seen with the point mutations. Again, no evidence for microtubule co-localization was observed. 0.5% Triton X-100 had no effect on the immunofluorescence pattern observed in cells transfected with the deletion mutant construct. Removal of more extensive regions from the NH₂ terminus of dynamin (constructs N-456 and N-651) abolished the punctate pattern (Table I).

Deletion of the COOH-terminal region of wild-type rat dynamin yielded a diffuse, cytoplasmic staining pattern (construct C-663, Fig. 4 d; construct C-794, Table I). However, deletion of the COOH-terminal 188 amino acids from the amino-terminal deletion construct N-272 (to produce construct N-272/C-663) abolished the punctate pattern produced by the NH₂-terminal deletion alone (Table I). Similarly, removal of the same COOH-terminal region from the point mutant construct K44E (to produce construct K44E/C-663) abolished the punctate/linear pattern (Fig. 4 c). Removal of a smaller region of the COOH terminus (to produce construct K44E/C-794) was insufficient to restore the diffuse wild-type immunofluorescence pattern (Fig. 4 b).

Effect of Transfection on Endocytosis

Examination of shibire mutant flies has revealed a defect in the formation of both coated and non-coated vesicles at the plasma membrane. However, despite the relatively close relationship in primary sequence between the Drosophila
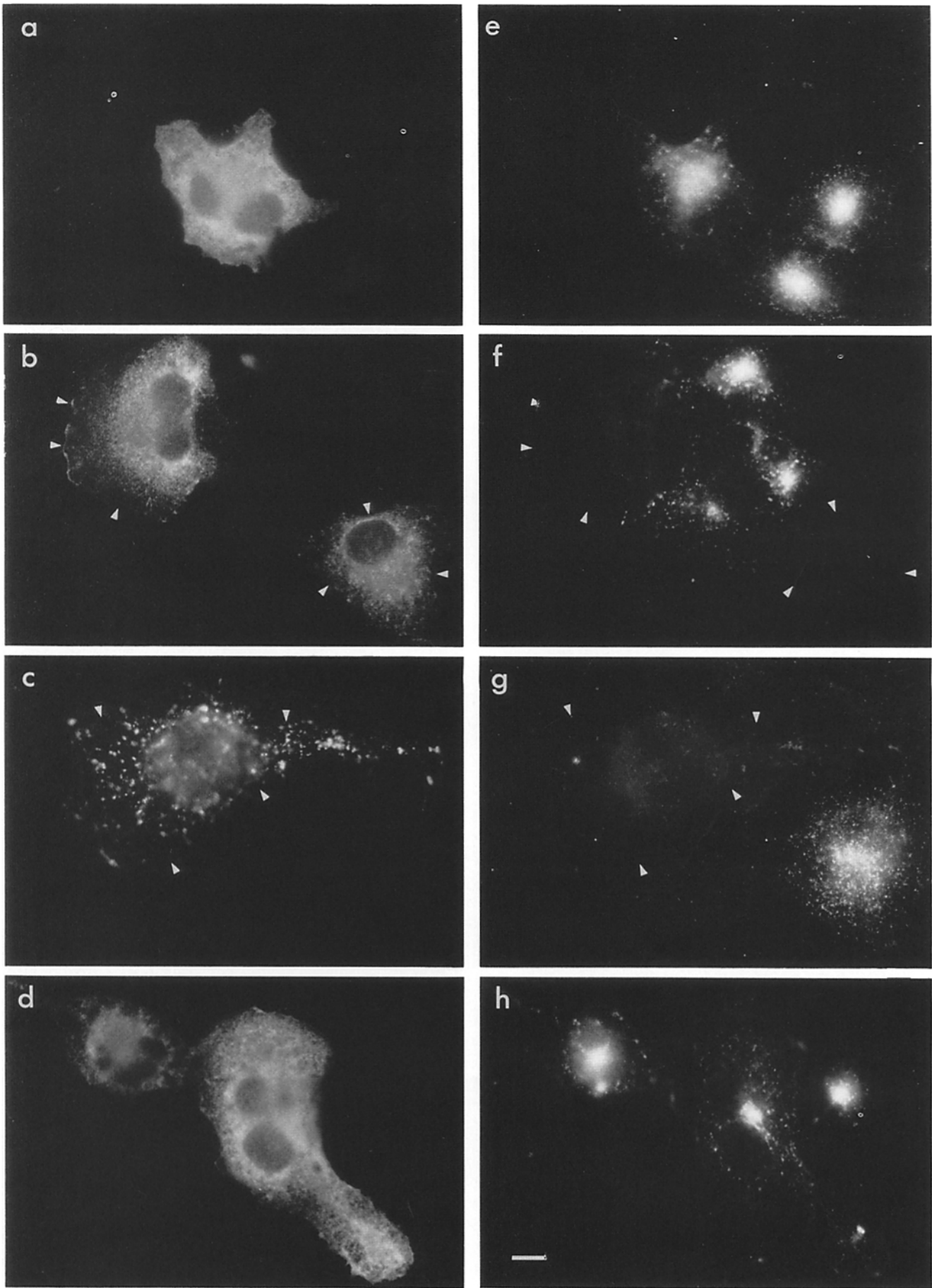
Figure 3. Mutant dynamin inhibits transferrin uptake. COS-7 cells were transfected with (*a* and *e*) the wild-type dynamin construct D-1; (*b* and *f*) the point mutant construct S45N; (*c* and *g*) the NH$_2$-terminal deletion construct N-272; or (*d* and *h*) the point mutant construct D208N, and exposed to 20 μ/ml FITC-transferrin for 60 min at 37°C. Left panels stained with anti-dynamin antibody: (*a*, *b*, *c*, and *d*) RA anti-peptide antibody. Right panels stained with FITC-transferrin. Cells transfected with S45N and N-272 mutant constructs and blocked in transferrin uptake are outlined by arrowheads. Bar, 10 μm.
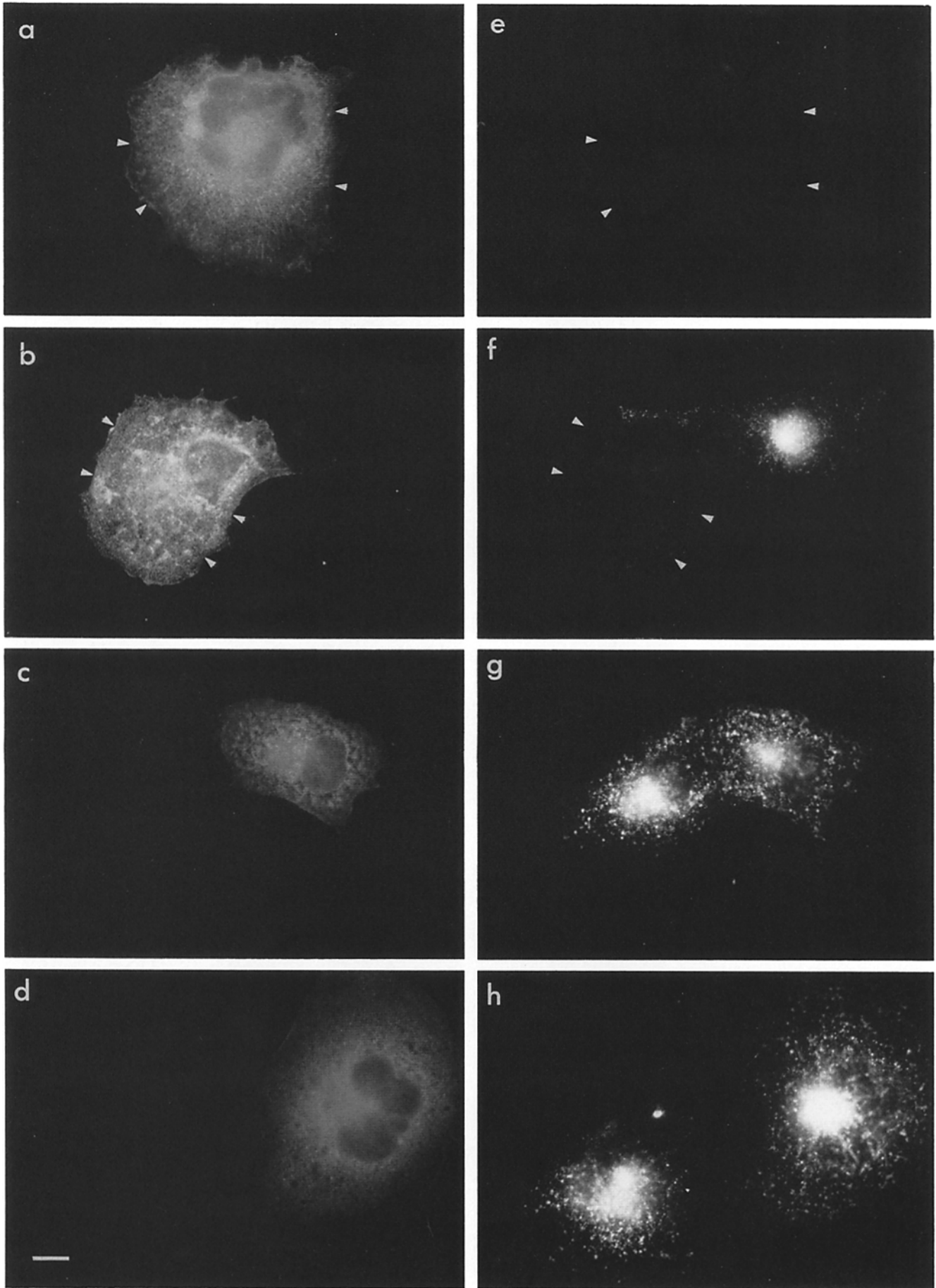
gene and rat dynamin, the extent to which their functions are related is unknown.

To test whether overexpression of wild-type or mutant dynamin indeed affected endocytosis, transfected cells were exposed to FITC-transferrin, fixed in formaldehyde, acetone extracted, and then counter-stained with antibody to dynamin. Clear uptake of labeled transferrin into vesicular elements located near the cell center was observed in non-transfected cells (Figs. 3–5), and in cells overexpressing wild-type dynamin (Fig. 3, a and e). However, transferrin uptake was abolished in cells transfected with the point mutant constructs K44E (Fig. 4, a and e) and S45N (Fig. 3, b and f), and the NH$_2$-terminal deletion N-272 (Fig. 3, c and g). In contrast to these results, no effect was observed in cells transfected with the point mutant construct D208N (Fig. 3, d and h).

As the COOH terminus of dynamin had been seen to affect the distribution of the protein, we assayed for the role of this domain in endocytosis. Removal of 188 codons from the 3′ end of construct K44E (to give construct K44E/C-663) completely reversed the inhibitory effect of the point mutation on transferrin uptake (Fig. 4, c and g). In contrast, removal of a smaller segment of the dynamin COOH terminus (construct K44E/C-794) had no effect (Fig. 4, b and f). Overexpression of the critical COOH-terminal segment (construct N-651) had no effect on transferrin uptake (Table I), nor did removal of the 3′ end from the wild-type construct (construct C-663; Fig. 4, d and h, Table I).

Under milder conditions of permeabilization (0.2% saponin) diffuse transferrin labeling of cells expressing the inhibitory K44E mutant form of dynamin was observed (Fig. 5, a and e, b and f). Of cells exhibiting the altered transferrin distribution pattern, 96% were seen to be transfected as judged by anti-dynamin labeling ($n = 102$). Conversely, of cells judged to be transfected by anti-dynamin labeling, 95% showed diffuse transferrin labeling ($n = 61$). In non-permeabilized transferrin-labeled cultures, a similar number of diffusely labeled cells was observed. The appearance of these cells was indistinguishable from that of the double-labeled cells, suggesting that the saponin did not substantially alter the transferrin distribution.

To determine whether the diffuse transferrin labeling was on the cell surface, cells exposed to FITC-transferrin were subsequently exposed to excess unlabeled transferrin in the cold to displace labeled transferrin from the surface. Under these conditions the surface labeling disappeared from the transfected cells, while endosome labeling in the control cells was unaffected (Fig. 5, c and g, d and h). Close examination of the apparent surface labeling pattern revealed very limited co-localization with structures observed in the same cells by anti-dynamin antibody. No clear indication of punctate cell surface staining consistent with the presence of transferrin in coated pits was observed, though this was likely to be obscured by the high level of diffuse staining.

Fluid-phase endocytosis was assayed by double labeling with anti-dynamin and FITC-dextran (Fig. 6). Cells transfected with the point mutant construct K44E showed clear evidence of fluid phase uptake (90% positive for transfected cells, $n = 40$; 97% positive for untransfected cells, $n = 235$). The linear dynamin-positive elements seen in some of these cells did not generally contain fluid phase marker. Double labeling for TRITC-transferrin and FITC-dextran was also examined in fixed but unextracted cells (data not shown). Cells showing diffuse transferrin staining were positive for fluid phase uptake at both early (15 min) and late (3 h) time points.

## Effects of Transfection on Other Subcellular Markers

To obtain further insight into the nature of the effects produced by mutant forms of dynamin, transfected cells were labeled with a variety of subcellular markers.

To investigate the role of dynamin in coated vesicle formation, cells transfected with wild-type or mutant rat dynamin were double labeled using antibodies to dynamin and to components of coated vesicles (reviewed in Brodsky, 1988; Pearse and Robinson, 1990; Keen, 1990). These included clathrin heavy chain, a component of all clathrin-coated pits and vesicles, α-adaptin, a component of plasma membrane-derived coated pits and vesicles (Robinson and Pearse, 1986), and γ-adaptin, which is associated with clathrin-coated structures of the TGN (Ahle et al., 1988).

In untransfected cells, clathrin heavy chain and α-adaptin were observed as small spots dispersed throughout the cytoplasm (see untransfected cell at left in Fig. 7 e), with a concentration of clathrin heavy chain spots also seen in the immediate vicinity of the Golgi apparatus. No effect on these distribution patterns was observed as the result of overexpression of wild-type dynamin (Fig. 7 a). On the other hand, those dynamin constructs which led to an altered dynamin staining pattern and affected transferrin uptake (point mutant constructs K44E, S45N, and the NH$_2$-terminal deletion construct N-272) all induced a redistribution of both clathrin and α-adaptin (Fig. 7, b and e, c and f; Table I). In most of these cells the clathrin heavy chain- and α-adaptin–positive spots were clustered into patches or aggregates. This effect was not directly correlated with the level of dynamin expression, as both weakly and strongly expressing cells showed the effect. No effect on the clathrin or α-adaptin distribution was observed with any of the other mutant constructs (Table I), including K44E/C-663 and N-272/C-663. Thus, deletion of the COOH-terminal region of dynamin restored the normal distribution of clathrin heavy chain and α-adaptin.

Examination of double-labeled mutant cells showed co-localization of dynamin and either clathrin heavy chain or α-adaptin in a few, but not most, spots. The clearest evidence for co-localization was observed in cells transfected with the NH$_2$-terminal deletion construct N-272 (e.g., Fig. 7, c and f). In cells transfected with the point mutant constructs K44E and S45N, the dynamin-positive linear structures

---

Figure 4. Effect of COOH-terminal deletions on dominant inhibitory effect of point mutant dynamin construct K44E. COS-7 cells were transfected with (a and e) the point mutant construct K44E; (b and f) the double mutant construct K44E/C-794; (c and g) the double mutant construct K44E/C-663; (d and h) the COOH-terminal deletion construct C-663, and exposed to transferrin as described in the previous figure. Left panels stained with anti-dynamin antibody: (a) RA anti–peptide antibody; (b, c, and d) R2 antibody. Right panels stained with FITC-transferrin. Cells transfected with constructs K44E and K44E/C-663 and blocked in transferrin uptake are outlined by arrowheads. Bar, 10 μm.
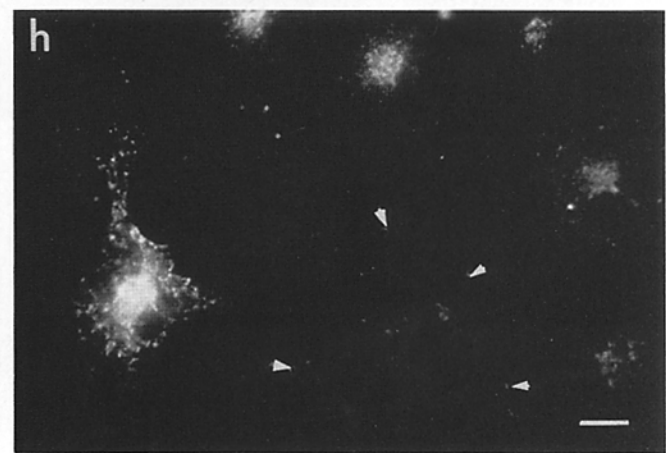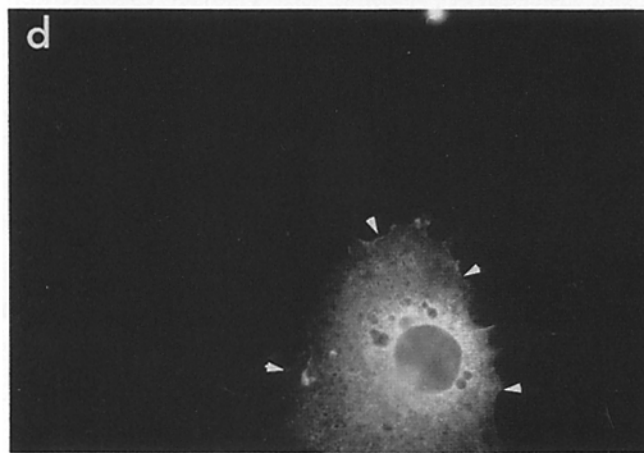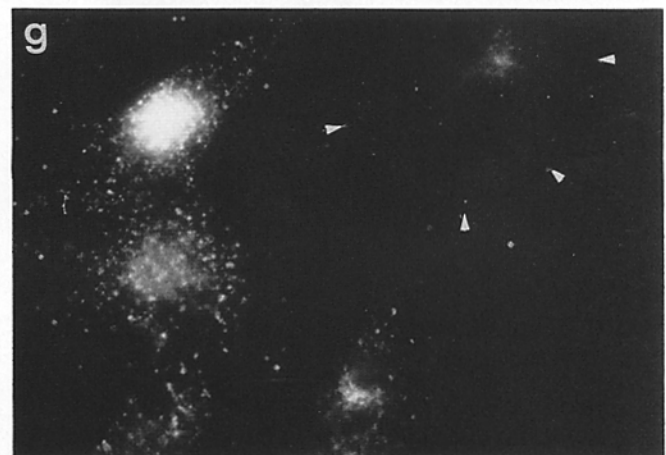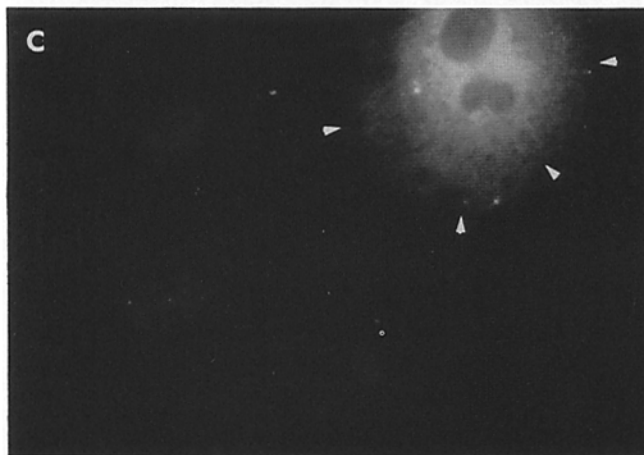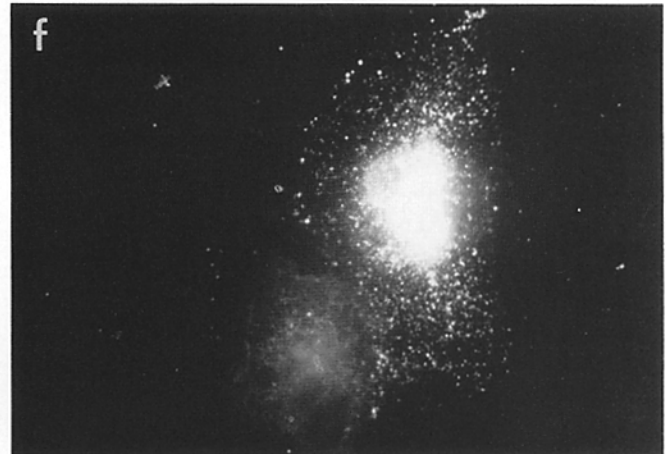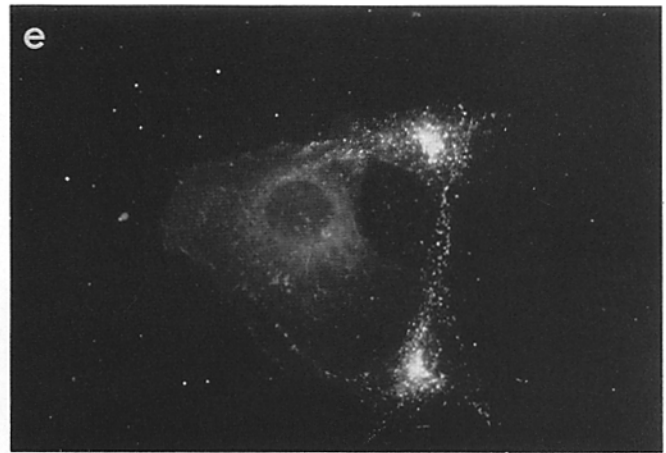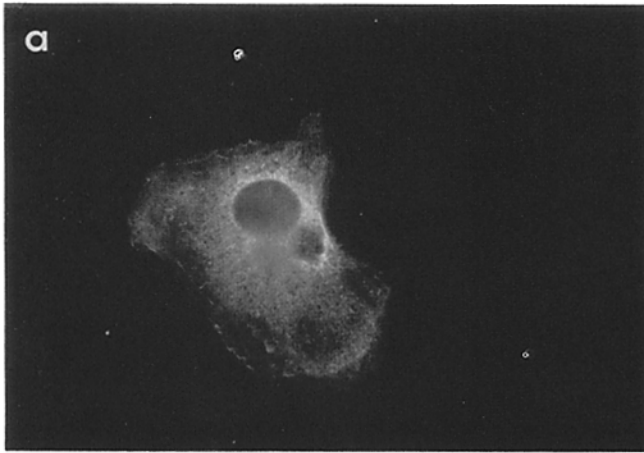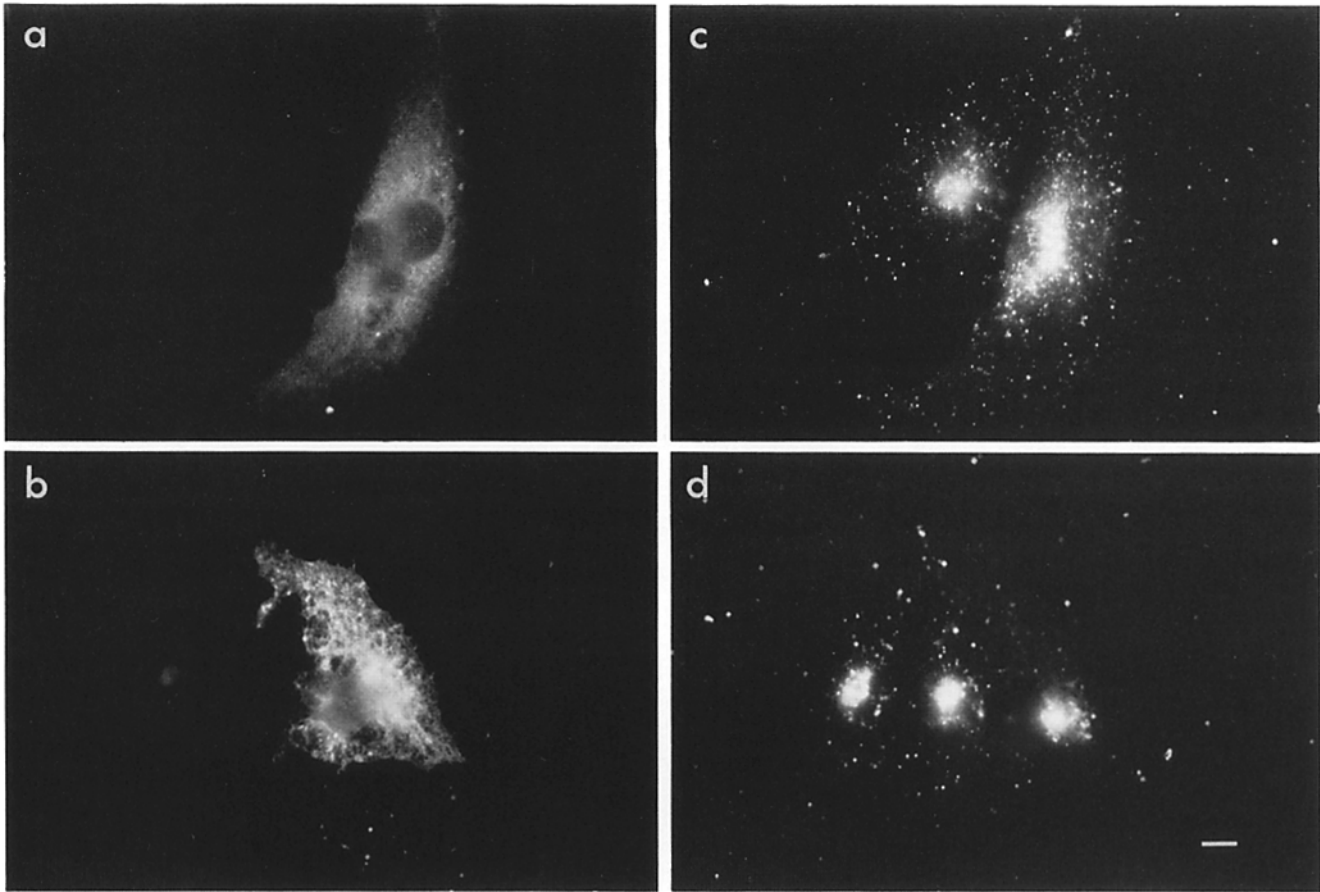
Figure 6. Fluid-phase endocytosis by cells expressing mutant dynamin (K44E). Cells were exposed to FITC-conjugated lysine-fixable dextran for 3–4 h at 37°C, and double-labeled with anti-dynamin. (*a* and *b*) anti-dynamin; (*c* and *d*) FITC-dextran. Bar, 10 μm.

were sometimes faintly reactive with the anti-clathrin and anti-α–adaptin antibodies.

Antibody to γ-adaptin also showed punctate staining, but with a concentration of immunoreactive spots in the Golgi region (Fig. 8; cf. Ahle et al., 1988). The distribution of this marker was unaffected in cells overexpressing either wild-type or mutant dynamin (Fig. 8). Similarly, no effect was observed in these cells staining for components of the Golgi apparatus (anti-58-kD antigen, β-COP), the ER (anti-BiP), actin (rhodamine-phalloidin), and intermediate filaments (anti-vimentin) (data not shown).

Discussion

We have over-expressed wild-type and mutant forms of rat dynamin to determine its subcellular distribution and to define its mechanism of action. Several distinct dominant inhibitory mutations in the GTPase domain blocked receptor-mediated endocytosis, an effect which could be reversed by deletion of the COOH-terminal basic, proline-rich region of the molecule. The mutant forms of dynamin exhibited altered distribution patterns within the cell, and induced

specific changes in the distribution of α-adaptin, but not γ-adaptin.

We saw no microtubule staining in unextracted cells over-expressing wild-type dynamin (Figs. 3–7). Depletion of ATP produced no detectable increase in microtubule binding, nor did mutations in the GTP-binding site. We did see occasional evidence for microtubule co-localization in detergent-extracted cells over-expressing wild-type dynamin. However, because this staining was weak and variable, and tended to be seen both in transfected cells as well as in neighboring non-transfected cells, this association may be non-physiological. Wild-type dynamin was diffusely distributed, consistent with the substantial proportion of brain dynamin which can be purification from cytosol (Shpetner and Vallee, 1989). Mutant forms of dynamin had a more particulate distribution, which may indicate that, as for some other GTPases such as ARF (Kahn et al., 1988), dynamin cycles between soluble and membrane-bound states.

The Role of Dynamin in Endocytosis

The present study firmly establishes an important role for

Figure 5. Distribution of transferrin in transfected cells. COS-7 cells were transfected with the point mutant dynamin construct K44E, exposed to transferrin, fixed, mildly permeabilized with saponin, and double-labeled with anti-dynamin. (*a–d*) anti-dynamin; (*e–h*) FITC-transferrin. (*a* and *e*, *b* and *f*) Cells were exposed to FITC-transferrin for 60 min at 37°C; (*c* and *g*, *d* and *h*) Cells were exposed to FITC-transferrin for 60 min at 37°C, chilled to 4°C and exposed to 1 mg/ml unlabeled transferrin for 60 min to chase surface labeling. Arrowheads outline transfected cells, which are seen to have very low residual FITC-transferrin after unlabeled transferrin chase. Bar, 10 μm.
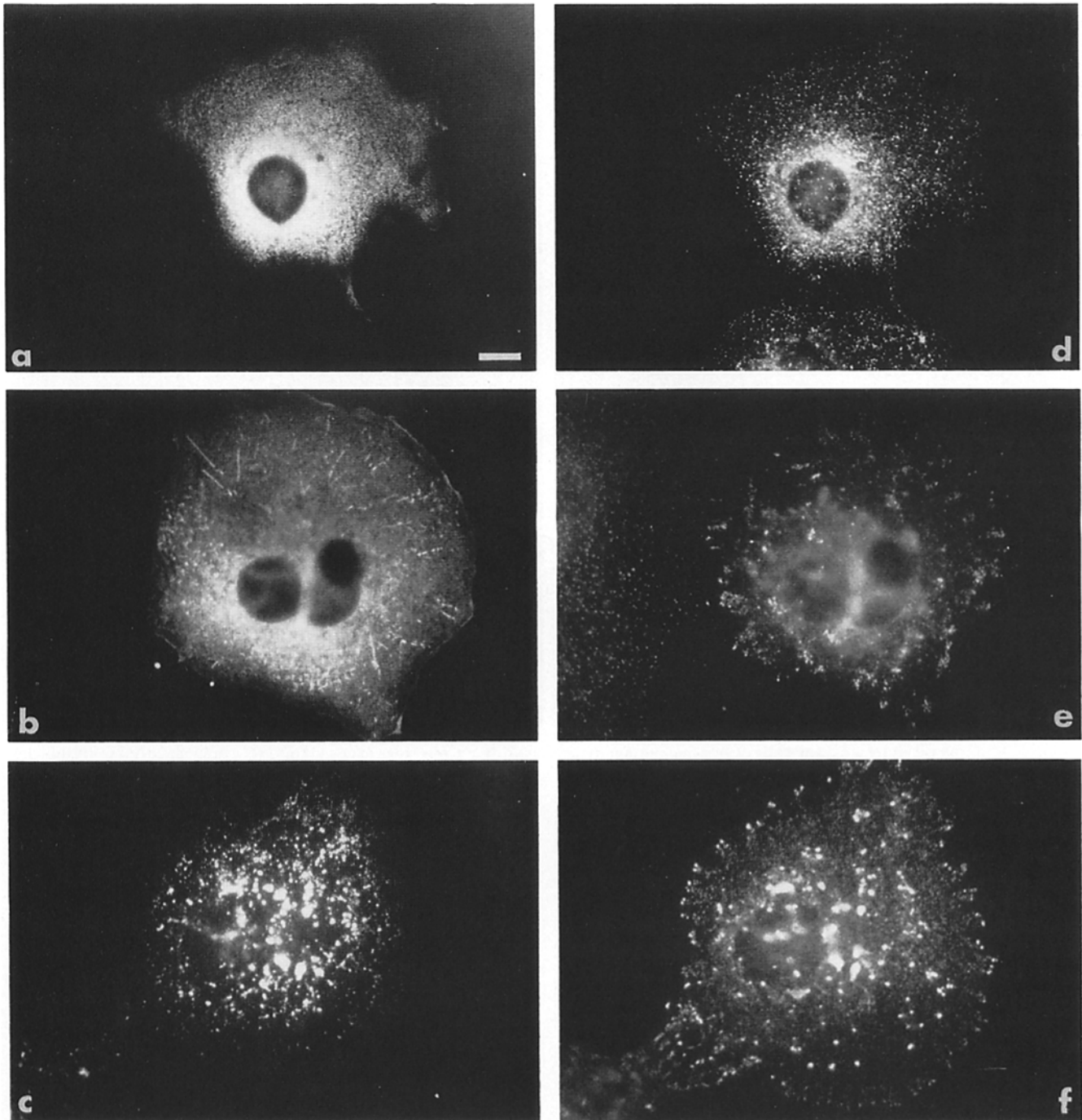
Figure 7. Mutant dynamin alters the distribution of clathrin heavy chain and α-adaptin. COS-7 cells were transfected with (*a* and *d*) the wild-type dynamin construct D-1; (*b* and *e*) the point mutant construct K44E; and (*c* and *f*) the NH₂-terminal deletion construct N-272. Antibodies used were: (*a* and *b*) protein A–purified RA anti-peptide antibody; (*c*) R2 anti-dynamin antibody; (*d*) anti-clathrin heavy chain; and (*e* and *f*) anti-α-adaptin. Note an example of an untransfected cell in *e* which has a normal α-adaptin distribution and is completely negative for endogenous dynamin using the RA antibody (*b*). Bar, 10 μm.

dynamin in receptor-mediated endocytosis. Two distinct point mutations and the NH₂-terminal deletion N-272 inhibited transferrin uptake into endosomes. Under mild permeabilization conditions transferrin was found in a diffuse distribution (Fig. 5, *a* and *e*, *b* and *f*). The labeled transferrin could be displaced by unlabeled ligand (Fig. 5, *c* and *g*, *d* and *h*), consistent with cell surface labeling in cells expressing the mutant forms of dynamin. Clear accumulation of the

labeled transferrin in coated pits was not observed, but further studies will be required to determine whether this reflects a block in receptor accumulation in the pit or merely an excess of diffuse receptor on the cell surface.

The mutant forms of dynamin clearly affected the distribution of coated vesicle components, a further indication that dynamin acts in conjunction with the coated vesicle pathway. The specific effect on α-adaptin indicates a role in the plasma
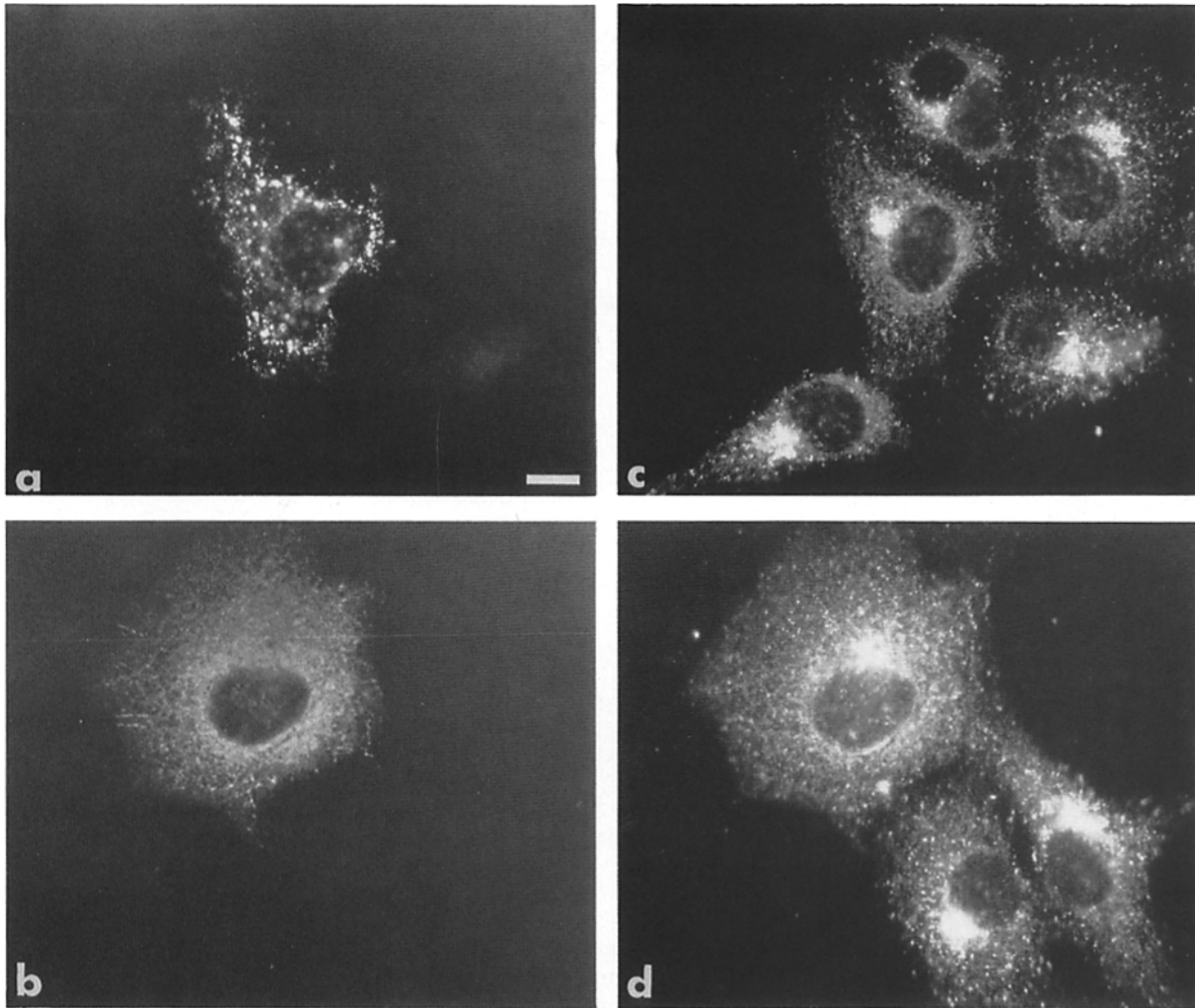
Figure 8. Mutant dynamin does not alter the distribution of γ-adaptin. COS-7 cells were transfected with (*a* and *c*) the NH$_2$-terminal deletion constructs N-272; or, (*b* and *d*) the point mutant construct S45N. Antibodies used were: (*a* and *b*) protein A–purified RA anti–peptide antibody diluted 1:200; (*c* and *d*) anti–γ-adaptin. Note that the distribution of γ-adaptin in the transfected cells is comparable to that in the neighboring non-transfected cells. Bar, 10 μm.

membrane-derived, but not the Golgi-derived coated vesicle pathway. This implies that, despite the obvious structural similarity between coated vesicles from the two subcellular regions, different regulatory elements operate in controlling their formation. The present data are consistent with other reports of differences in the behavior of α- and γ-adaptin (Robinson and Kreis, 1992), and further underscore the importance of the adaptins in specifying the functional diversity of coated vesicles. An attractive hypothesis is that α-adaptin itself is responsible for targeting dynamin to the endocytic pathway via either a direct or indirect interaction, and it will be of great interest to test this possibility. Whether other dynamin-related GTPases play an equivalent role in the formation of coated vesicles from the TGN is unknown. Such a role is consistent with the properties of the yeast gene VPS1 (Rothman et al., 1990), though a specific involvement for VPS1 in coated vesicle formation has not been evaluated. Present efforts are directed at identifying a comparable protein in mammalian cells.

The mutant dynamin constructs were found to block receptor-mediated, but not fluid-phase endocytosis. This re-

sult conflicts with observations of cells from *shi*^{ts} flies under restrictive conditions (Kosaka and Ikeda, 1983*b*; Kessell et al., 1989). In these studies fluid-phase uptake was judged to be blocked using a quantitative electron microscopic assay; receptor-mediated endocytosis was not examined.

While this apparent contradiction may ultimately be ascribed to a difference in the kinetic sensitivity of the assays used, there are at least two more interesting explanations for a real difference between our results and those of the earlier studies on *shibire*. First, our experiments involve a single isoform of rat dynamin. Conceivably, mutations in the isoform involved in the present study may not affect all aspects of endocytosis. There is also evidence for endocytosis in mammalian cells via non-clathrin–mediated pathways (for example, Sandvig and van Duers, 1990; Rothberg et al., 1990, 1992). While it is not known whether dynamin is involved in these pathways, the mutant constructs defined here may be of great value in discriminating between pathways experimentally. We have no doubt that that fraction of fluid-phase endocytosis representing entrapment during coated vesicle internalization is inhibited in our cells; our results

Table I. Dynamin Constructs

Construct		Dynamin distribution	α-Adaptin distribution	Tf uptake
D-1	1-851	Diffuse	Disperse	+
K44E	1-851	Punctate, Linear	Clustered	-
S45N	1-851	Punctate, Linear	Clustered	-
D208N	1-851	Diffuse	Disperse	+
K44E/C-794	1-794	Punctate, Linear	Clustered	-
K44E/C-663	1-663	Diffuse	Disperse	+
C-794	1-794	Diffuse	Disperse	
C-663	1-663	Diffuse	Disperse	+
N-272	272-851	Punctate	Clustered	-
N-272/C-663	272-663	Diffuse	Disperse	+
N-456	456-851	Diffuse	Disperse	
N-651	651-851	Diffuse	Disperse	+

Point mutations are indicated by an X in one of three GTP-binding consensus sequence elements, represented by vertical tick marks. Effect of mutations on dynamin and α-adaptin distributions, and FITC-transferrin uptake are indicated. Constructs with abnormal dynamin distribution showed clustered α-adaptin spots and were defective in transferrin uptake. (Blank spaces indicate not determined.)

only indicate that significant fluid-phase uptake still occurs in cells expressing mutant dynamin.

Role of GTP in Dynamin Function

The mutations in the GTP-binding consensus sequence elements of dynamin were based on ras mutations for which comparable dynamin mutations could be designed. In preliminary experiments we found that ^{32}P-labeled GTP dissociated from dynamin during immunoprecipitation (data not shown), making direct analysis of the state of the dynamin-bound nucleotide difficult. This distinction from the small GTPases is likely to be related to the other distinctive characteristics of the dynamin GTPase, such as its relatively high K_m for GTP hydrolysis and high basal GTPase rate (Shpetner and Vallee, 1992). It is also noteworthy that evidence to date on the dynamin-related protein Mx has re-

Table II. Diagram of Dynamin Point Mutations

	I	II	III
	GXXXXGKS	DXXG	N/TKXD
Dynamin	GDQSSGKS	DLPG	TKPD
K44E	GDQSSG**E**S	DLPG	TKPD
S45N	GDQSSGK**N**	DLPG	TKPD
D208N	GDQSSGKS	DLPG	TKP**N**

GTP-binding consensus sequence elements are shown at top (from Bourne et al., 1991). Mutated amino acids are underlined and in bold.

vealed a similarly high basal GTPase activity and a very low affinity for guanine nucleotides (Nakayama et al., 1991; Horisberger, 1992; Staeheli, 1993).

Nonetheless, the phenotype induced by those ras mutations upon which the present mutations were based offers some insight into the possible role of GTP in the mechanism of action of dynamin. Mutation S45N in dynamin corresponds to mutation S17N in H-ras. This mutation specifically inhibits GTP binding, without significantly affecting the affinity of ras for GDP (Feig and Cooper, 1986), and produces a dominant inhibitory phenotype. Thus, the simplest interpretation of the dynamin S45N phenotype is that the observed inhibition of transferrin uptake results from an increase in the fraction of GDP-bound dynamin.

The K44E mutation in dynamin was based on the K16N mutation in H-ras (Sigal et al., 1986). The ras mutation had an inhibitory phenotype, but, unlike S17N, showed a decreased affinity for both GTP and GDP, suggesting that it was the empty state of the protein which was inhibitory. As for S17N, it was reasoned from the dominant character of the mutation that it formed a dead-end complex with a protein with which wild-type ras interacted only transiently.

That S45N and K44E in dynamin are both inhibitory to transferrin uptake suggests that they have effects on dynamin comparable to those of the inhibitory ras mutations. In view of the different biochemical properties of S17N and K16N in ras, it appears that both the GDP-bound state and the empty state can have similar phenotypic effects. In the case of dynamin this view is consistent with the dominant inhibitory

effect of the NH₂-terminal deletion mutant N272 in dynamin which may correspond to the empty state, in view of the complete absence of the GTP-binding domain.

In contrast to the inhibitory mutations, the dynamin mutation D208N, which was based on the oncogenic mutations D119N and D119A in ras (Feig et al., 1986; Sigal et al., 1986), had no effect on transferrin uptake. D119A in ras is oncogenic, implying that, while the affinity for both GDP and GTP is reduced 20-fold (Sigal et al., 1986), the life-time of the GTP state is increased. This has been interpreted in terms of the formation of an activating, rather than a dead-end complex with other cellular proteins. In the case of dynamin, the D208N mutation has no apparent phenotype, suggesting that the GTP-bound state plays a different role in the dynamin and ras activity cycles. However, we can conclude that, as in the case of ras, formation of a dead-end inhibitory complex by this mutant form of dynamin is unlikely, but further work will be needed define the biochemical effects of the D208N mutation more fully.

Recent analysis of endocytosis in lysed cell model systems have differed regarding a possible role for GTP (Lin et al., 1991; Schmid and Smythe, 1991; but see Carter et al., 1993). However, the effect of mutations in the GTP-binding site of dynamin observed in the present study clearly indicate such a role in the initial stages of endocytosis. The difference in the results of the several studies could be explained if dynamin served to assure the efficiency or fidelity of endocytosis, rather than playing an obligatory role in the process. While the present experiments reveal a complete block in transferrin uptake in cells transfected with mutant forms of dynamin, this result could reflect poisoning of an early endocytic intermediate by the mutant protein. The absence of dynamin could, conceivably, allow endocytosis to proceed, but with lower efficiency.

The Role of the Dynamin COOH Terminus

We find that deletion of the COOH-terminal portion of dynamin reverses the effects of the K44E and N-272 mutations (Fig. 7; Table I), indicating this domain to be critical for dynamin activity. All aspects of the dominant inhibitory phenotype were reversed by removal of the COOH terminus — the inhibition of transferrin uptake, the more particulate distribution of dynamin, and the alteration in the distribution of clathrin and α-adaptin. This serves as further indication that these phenomena are linked, and suggests that the novel dynamin-containing structures are real intermediates in the dynamin functional cycle rather than abnormal protein aggregates. We surmise that it is through its COOH terminus that dynamin interacts with either upstream or downstream targets. While it is also possible that removal of the dynamin COOH terminus results in the improper folding of the molecule, this seems unlikely in view of the recent results of proteolytic modification of dynamin obtained in our laboratory. Removal of an ~7–9-kD portion of the molecule at the extreme COOH terminus by exposure to papain renders the protein incapable of binding to microtubules (Herskovits, J. S., C. C. Burgess, H. S. Shpetner, R. B. Vallee, manuscript submitted for publication). The basal dynamin GTPase activity is unaffected by this treatment, but stimulation by microtubules is abolished. While a role for microtubules per se in dynamin function is not obvious from the

present study, these results together identify the dynamin COOH terminus as an important regulatory domain.

It is of some interest that the greatest deviation in primary structure between isoforms of *shibire* and between *shibire* and rat dynamin occurs within the COOH-terminal 100 amino acids. Alignment of dynamin with other members of its family (Obar et al., 1990) also reveals this region to extend beyond the COOH termini of VPS1/SPO15, Mx and MGM-1. This suggests that the dynamin COOH terminus specifies a regulatory interaction unique to this protein. In addition, the existence of at least two forms of the COOH terminus in *Drosophila* suggests that either the affinity or the specificity of the interaction of dynamin with upstream or downstream elements is defined within this region. We note that overexpression of the COOH-terminal domain by itself had no obvious phenotypic effect. Therefore, this region alone does not appear to compete effectively for dynamin binding sites within the cell. Nonetheless, identification of the COOH-terminal region of dynamin as a functional domain should be of great value in identifying dynamin-interacting proteins biochemically.

References

Ahle, S., A. Mann, U. Eichelsbacher, and E. Ungewickell. 1988. Structural relationships between clathrin assembly proteins from the Golgi and the plasma membrane. *EMBO (Eur. Mol. Biol. Organ.) J.* 7:919–929.

Aruffo, A. 1991. Transient expression of proteins using COS cells. *In* Current Protocols in Molecular Biology. F. M. Ausubel, R. Brent, R. E. Kingston, D. D. Moore, J. D. Seidman, J. A. Smith, and K. Struhl, editors. Greene Publications and Wiley-Interscience, New York. 8.5.1–8.5.9.

Balch, W. E. 1990. Small GTP-binding proteins in vesicular transport. *Trends Biol. Sci.* 15:473–477.

Bamburg, J. R., E. M. Shooter, L. Wilson. 1973. Developmental changes in microtubule protein of chick brain. *Biochemistry.* 12:1476–1482.

Bourne, H. R., D. A. Sanders, and F. McCormick. 1991. The GTPase superfamily: conserved structure and molecular mechanism. *Nature (Lond.).* 349:117–127.

Brodsky, F. M. 1988. Living with clathrin: its role in intracellular membrane traffic. *Science (Wash. DC).* 242:1396–1402.

Carter, L. L., T. E. Redelmeier, L. A. Woolenweber, and S. L. Schmid. 1993. Multiple GTP-binding proteins participate in clathrin-coated vesicle-mediated endocytosis. *J. Cell Biol.* 120:37–45.

Chen, M. S., R. A. Obar, C. C. Schroeder, T. W. Austin, C. A. Poodry, S. A. Wadsworth, and R. B. Vallee. 1991. Multiple forms of dynamin are encoded by *shibire*, a *Drosophila* gene involved in endocytosis. *Nature (Lond.).* 351:583–586.

Chen, M. S., C. C. Burgess, R. B. Vallee, and S. C. Wadsworth. 1992. Developmental stage- and tissue-specific expression of *shibire*, a *Drosophila* Gene Involved in Endocytosis. *J. Cell Sci.* 103:619–628.

Cormack, B. 1991. Mutagenesis by the polymerase chain reaction. *In* Current Protocols in Molecular Biology, F. M. Ausubel, R. Brent, R. E. Kingston, D. D. Moore, J. D. Seidman, J. A. Smith, and K. Struhl, editors. Greene Publications and Wiley-Interscience, New York. 8.5.1–8.5.9.

Doxsey, S. J., F. M. Brodsky, G. S. Blank, and A. Helenius. 1987. Inhibition of endocytosis by anti-clathrin antibodies. *Cell.* 50:453–463.

Draper, R. K., Y. Goda, F. M. Brodsky, and S. R. Pfeffer. 1990. Antibodies to clathrin inhibit endocytosis but not recycling to the trans-Golgi network *in vitro. Science (Wash. DC).* 248:1539–1541.

Farnsworth, C. L., and L. A. Feig. 1991. Dominant inhibitory mutations in the Mg^{2+}-binding site of ras^H prevent its activation by GTP. *Mol. Cell. Biol.* 11:4822-4829.

Feig, L. A., B.-T. Pan, T. M. Roberts, and G. M. Cooper. 1986. Isolation of ras GTP-binding mutants using an *in situ* colony-binding assay. *Proc. Natl. Acad. Sci. USA.* 83:4607-4611.

Feig, L. A., and G. M. Cooper. 1988. Inhibition of NIH 3T3 cell proliferation by a mutant ras protein with preferential affinity for GDP. *Mol. Cell. Biol.* 8:3235-3243.

Flucher, B. E., M. Terasaki, H. Chin, T. J. Beeler, and M. P. Daniels. 1991. Biogenesis of transverse tubules in skeletal muscle in vitro. *Dev. Biol.* 145:77-90.

Grigliatti, T. A., L. Hall, R. Rosenbluth, and D. T. Suzuki. 1973. Temperature-sensitive mutations in *Drosophila melanogaster* XIV. A selection of immobile adults. *Mol. Genet.* 120:107-114.

Honig, M. G., and R. E. Hume. 1986. Fluorescent carbocyanine dyes allow living neurons of identified origin to be studied in long-term cultures. *J. Cell Biol.* 193:171-187.

Horisberger, M. A., and M. C. Gunst. 1991. Interferon-induced proteins: identification of Mx proteins in various mammalian species. *Virology.* 180:185-190.

Horisberger, M. A., P. Staeheli, and O. Haller. 1983. Interferon induces a unique protein in mouse cells bearing a gene for resistance to influenza virus. *Proc. Natl. Acad. Sci. USA.* 80:1910-1914.

Horisberger, M. A., G. K. McMaster, H. Zeller, M. G. Wathelet, J. Dellis, and J. Content. 1990. Cloning and sequence analysis of cDNAs for interferon- and virus-induced human Mx proteins reveal that they contain putative guanine nucleotide-binding sites. *J. Virol.* 64:1171-1181.

Horisberger, M. A. 1992. Interferon-induced human protein MxA is a GTPase which binds transiently to cellular proteins. *J. Virol.* 66:4705-4709.

Jones, B., and W. Fangman. 1992. Mitochondrial DNA maintenance in yeast requires a protein containing a region related to the GTP-binding domain of dynamin. *Genes & Dev.* 6:380-389.

Kahn, R. A., C. Goddard, and M. Newkirk. 1988. Chemical and immunological characterization of the 21-kDa ADP-ribosylation factor of adenylate cyclase. *J. Biol. Chem.* 263:8282-8287.

Kahn, R. A., F. G. Kern, J. Clark, E. P. Gelmann, and C. Rulka. 1991. Human ADP-ribosylation factors. *J. Biol. Chem.* 266:2606-2614.

Kahn, R. A., P. Randazzo, T. Serafini, O. Weiss, C. Rulka, J. Clark, M. Amherdt, P. Roller, L. Orci, and J. E. Rothman. 1992. The amino terminus of ADP-ribosylation factor (ARF) is a critical determinant of ARF activities and is a potent and specific inhibitor of protein transport. *J. Biol. Chem.* 267:13039-13046.

Keen, J. H. 1990. Clathrin and associated assembly and disassembly proteins. *Ann. Rev. Biochem.* 59:415-438.

Kim, Y.-T., and C.-F. Wu. 1990. Allelic interactions at the *shibire* locus of *Drosophila*: effects on behavior. *J. Neurogenet.* 7:1-14.

Koenig, J. H., K. Saito, and K. Ikeda. 1983. Reversible control of synaptic transmission in a single gene mutant of *Drosophila melanogaster*. *J. Cell Biol.* 96:1517-1522.

Koenig, J. H., and K. Ikeda. 1989. Disappearance and reformation of synaptic vesicle membrane upon transmitter release observed under reversible blockage of membrane retrieval. *J. Neurosci.* 9:3844-3860.

Kessell, I., B. Holst, and T. F. Roth. 1989. Membranous intermediates in endocytosis are labile, as shown in a temperature-sensitive mutant. *Proc. Natl. Acad. Sci. USA.* 86:4968-4972.

Kosaka, T., and K. Ikeda. 1983a. Possible temperature-dependent blockage of synaptic vesicle recycling induced by a single gene mutation in *Drosophila*. *J. Neurobiol.* 14:207-225.

Kosaka, T., and K. Ikeda. 1983b. Reversible blockage of membrane retrieval and endocytosis in the garland cell of the temperature-sensitive mutant of *Drosophila melanogaster*, *shibire^{ts1}*. *J. Cell Biol.* 97:499-507.

Laemmli, U. K. 1970. Cleavage of structural proteins during the assembly of the head of the bacteriophage T4. *Nature (Lond.).* 227:680-685.

Lin, H. C., M. S. Moore, D. A. Sanan, and R. G. W. Anderson. 1991. Reconstitution of clathrin-coated pit budding from plasma membranes. *J. Cell Biol.* 114:881-892.

Lin X., and C. A. Collins. 1992. Immunolocalization of cytoplasmic dynein to lysosomes in cultured cells. *J. Cell Biol.* 101:125-137.

Lippincott-Schwartz, J., J. G. Donaldson, A. Schweizer, E. G. Berger, H.-P. Hauri, L. C. Yuan, and R. D. Klausner. 1990. Microtubule-dependent retrograde transport of proteins in the ER in the presence of brefeldin A suggests an ER recycling pathway. *Cell.* 60:821-836.

Lippincott-Schwartz, J., L. C. Yuan, C. Tipper, M. Amherdt, L. Orci, and R. D. Klausner. 1991. Brefeldin A's effects on endosomes, lysosomes, and TGN suggest a general mechanism for regulating organelle structure and membrane traffic. *Cell.* 67:601-616.

Masur, S. K., Y.-T. Kim, and C.-F. Wu. 1990. Reversible inhibition of endocytosis in cultured neurons from the *Drosophila* temperature-sensitive mutant, *shibire*. *J. Neurogenet.* 6:191-206.

Nakata, T., A. Iwamoto, Y. Noda, R. Takemura, H. Yoshikura, and N. Hirokawa. 1991. Predominant and developmentally regulated expression of dynamin in neurons. *Neuron.* 7:461-469.

Nakayama, M., K. Nagata, A. Kato, and A. Ishihama. 1991. Interferon-inducible mouse Mx1 protein that confers resistance to influenza virus is a GTPase. *J. Biol. Chem.* 266:21404-21408.

Obar, R. A., C. A. Collins, J. A. Hammarback, H. S. Shpetner, and R. B. Vallee. 1990. Molecular cloning of the microtubule-associated mechanochemical enzyme dynamin reveals homology with a new family of GTP-binding proteins. *Nature (Lond.).* 347:256-261.

Olmsted, J. B. 1981. Affinity purification of antibodies from diazotized paper blots of heterogeneous protein samples. *J. Biol. Chem.* 256:11955-11957.

Pai, E. F., W. Kabasch, U. Krengel, K. C. Holmes, J. John, and A. Wittinghofer. 1989. Structure of the guanine-nucleotide binding domain of the H-ras oncogene product p21 in the triphosphate conformation. *Nature (Lond.).* 341:209-214.

Pai, E. F., U. Krengel, G. A. Petsko, R. S. Goody, W. Kabasch, and A. Wittinghofer. 1990. Refined crystal structure of the triphosphate conformation of H-ras p21 at 1.35 Å resolution: implications for the mechanism of GTP hydrolysis. *EMBO (Eur. Mol. Biol. Organ.) J.* 9:2351-2359.

Pearse, B. M. F., and M. S. Robinson. 1990. Clathrin, adaptors, and sorting. *Ann. Rev. Cell Biol.* 6:151-171.

Pfister, K. K., M. C. Wagner, D. L. Stenoien, S. T. Brady, and G. S. Bloom. 1989. Monoclonal antibodies to kinesin heavy and light chains stain vesicle-like structures, but not microtubules, in cultured cells. *J. Cell Biol.* 108:1453-1463.

Poodry, C. A., and L. Edgar. 1979. Reversible alterations in the neuromuscular junctions of *Drosophila melanogaster* bearing a temperature-sensitive mutation, *shibire*. *J. Cell Biol.* 81:520-527.

Robinson, M. S., and B. M. F. Pearse. 1986. Immunofluorescence localization of 100K coated vesicle proteins. *J. Cell Biol.* 102:48-54.

Robinson, M. S., and T. E. Kreis. 1992. Recruitment of coat proteins onto Golgi membranes in intact and permeabilized cells: effects of brefeldin A and G protein activators. *Cell.* 69:129-138.

Rothberg, K. G., Y.-S. Ying, J. F. Kolhouse, B. A. Kamen, and R. G. W. Anderson. 1990. The glycophospholipid-linked folate receptor internalizes folate without entering the clathrin-coated pit endocytic pathway. *J. Cell Biol.* 110:637-649.

Rothberg, K. G., J. E. Heuser, W. C. Donzell, Y.-S. Ying, J. R. Glenney, and R. G. W. Anderson. 1992. Caveolin, a protein component of caveolae membrane coats. *Cell.* 68:673-682.

Rothman, J. H., C. K. Raymond, T. Gilbert, P. J. O'Hara, and T. H. Stevens. 1990. A putative GTP binding protein homologous to interferon-inducible Mx proteins performs an essential function in yeast protein sorting. *Cell.* 61:1063-1074.

Sandvig, K., and B. Van Deurs. 1990. Selective modulation of the endocytic uptake of ricin and fluid phase markers without alteration in transferrin endocytosis. *J. Biol. Chem.* 265:6382-6388.

Sanger, F., S. Nicklen, and A. Coulson. 1977. DNA sequencing with chain-terminating inhibitors. *Proc. Natl. Acad. Sci. USA.* 74:5463-5467.

Scaife, R., and R. L. Margolis. 1990. Biochemical and immunochemical analysis of rat brain dynamin interaction with microtubules and organelles in vivo and in vitro. *J. Cell Biol.* 111:3023-3033.

Schmid, S. L., and E. Smythe. 1991. Stage-specific assays for coated pit formation and coated vesicle budding *in vitro*. *J. Cell Biol.* 114:869-880.

Shpetner, H. S., and R. B. Vallee. 1989. Identification of dynamin, a novel mechanochemical enzyme that mediates interactions between microtubules. *Cell.* 59:421-432.

Shpetner, H. S., and R. B. Vallee. 1992. Dynamin is a GTPase stimulated to high levels of activity by microtubules. *Nature (Lond.).* 355:733-735.

Sigal, I. S., J. B. Gibbs, J. S. D'Alonzo, G. L. Temeles, B. S. Wolanski, S. H. Socher, and E. M. Scolnick. 1986. Mutant ras-encoded proteins with altered nucleotide binding exert dominant biological effects. *Proc. Natl. Acad. Sci. USA.* 83:952-956.

Staeheli, P., O. Haller, W. Boll, H. Lindenmann, and C. Weissmann. 1986. Mx protein: constitutive expression in 3T3 cells transformed with cloned Mx cDNA confers selective resistance to influenza virus. *Cell.* 44:147-158.

Staeheli, P. 1993. The GTPase superfamily. *In* Ciba Foundation Symposium. In press.

Towbin, J., T. Staehelin, and J. Gordon. 1979. Electrophoretic transfer of proteins from polyacrylamide gels to nitrocellulose sheets: procedure and some applications. *Proc. Natl. Acad. Sci. USA.* 76:4350-4354.

Vallee, R. B. 1986. Purification of brain microtubules and microtubule-associated proteins 1 using taxol. *Methods Enzymol.* 134:104-116.

van der Bliek, A. M., and E. M. Meyerowitz. 1991. Dynamin-like protein encoded by the *Drosophila shibire* gene associated with vesicular traffic. *Nature (Lond.).* 351:411-414.

Walworth, N. C., P. Brennwald, A. K. Kabcenell, M. Garrett, and P. Novick. 1992. Hydrolysis of GTP by Sec4 protein plays an important role in vesicular transport and is stimulated by a GTPase-activating protein in *Saccharomyces cerevisiae*. *Mol. Cell. Biol.* 12:2017-2028.

Yeh, E., R. Driscoll, M. Coltrera, A. Olins, and K. Bloom. 1991. A dynamin-like protein encoded by the yeast sporulation gene SPO15. *Nature (Lond.).* 349:713-715.